Journal of Luminescence 143 (2013) 498–502

Contents lists available at SciVerse ScienceDirect

Journal of Luminescence

journal homepage: www.elsevier.com/locate/jlumin

Photoluminescence of Se-related oxygen deficient center in ion-implanted silica films

A.F. Zatsepin [a,*], E.A. Buntov [a], V.A. Pustovarov [a], H.-J. Fitting [b]

[a] Ural Federal University, Mira 19, 620002 Ekaterinburg, Russia
[b] Department of Physics, University of Rostock, Universitätsplatz 3, D-18051 Rostock, Germany

ARTICLE INFO

Article history:
Received 20 February 2013
Received in revised form
26 April 2013
Accepted 30 May 2013
Available online 6 June 2013

Keywords:
Silica films
Ion implantation
Selenium
Photoluminescence
Oxygen deficient centers

ABSTRACT

The results of low-temperature time-resolved photoluminescence (PL) investigation of thin SiO_2 films implanted with Se^+ ions are presented. The films demonstrate an intensive PL band in the violet spectral region, which is attributed to the triplet luminescence of a new variant of selenium-related oxygen deficient center (ODC). The main peculiarity of the defect energy structure is the inefficient direct optical excitation. Comparison with spectral characteristics of isoelectronic Si-, Ge- and SnODCs show that the difference in electronic properties of the new center is related to ion size factor. It was established that the dominating triplet PL excitation under VUV light irradiation is related to the energy transfer from SiO_2 excitons. A possible model of Se-related ODC is considered.

1. Introduction

Amorphous silicon dioxide (SiO_2) and its low-dimensional modifications are of technological importance in the growing fields of optoelectronics and photonics [1]. Complex silica-based functional materials, including structures containing semiconductor quantum dots, are often created by means of ion implantation. Required compatibility with the current technology in the semiconductor industry induces an extensive research on Si-based emitting materials in which photoluminescence (PL) properties of Si-, Ge-, and Sn-implanted SiO_2 layers were studied [2–4]. Such ion-beam synthesis is inevitably accompanied by generation of point defects which affect the optical properties of the host matrix. However detailed information concerning the point defects nature and energy parameters is required in order to understand the regularities and mechanisms of optical properties formation for SiO_2-based structures [5].

The majority of group IV elements: silicon (Si), germanium (Ge) and tin (Sn) are known to form ODC-type defects in SiO_2 matrix. Among the optically active defects the most studied are silicon and germanium oxygen deficient centers (SiODC and GeODC) [5]. The models of neutral oxygen vacancy ≡Si–Si≡ (≡Ge–Ge≡) and twofold-coordinated silicon =Si: (germanium =Ge:) had been proposed for them. Though the former model has not been totally disproven, the latter is now chosen by the most of authors [6]. The principal optical bands related to these defects refer to the so-called B-type activity, consisting of an optical absorption (OA) band, centered at 5 eV, and of two photoluminescence (PL) emissions centered at 4.2–4.4 and 2.7–3.1 eV [6]. A similar optical activity is also present in Sn-doped silica and has been attributed to SnODC centers [2,3,8–10]. Some authors have shown that the UV optical absorption (OA) of Sn-doped silica is dominated by a band peaked at 4.9 eV, which excites two photoluminescence (PL) emissions at 4.1 eV, decaying in few nanonseconds, and at 3.2 eV, decaying in few microseconds [8–10]. The overall B-type activity has been associated with a single structural model: the twofold coordinated atom also indicated as =Sn: [6].

Thus the oxygen deficient centers of the isoelectronic series (Si, Ge and Sn) demonstrate similar spectroscopic and structural features. But is this list exhaustive? Though this group of elements contains also the carbon (C) and lead (Pb), they are not presently known to form ODC-type defect. The Pb atom seems too large and heavy (207 amu) to substitute silicon in the silica lattice, while carbon may react with silicon and oxygen to form stable compounds and therefore it is unlikely to create substitution defects. Nevertheless one might imagine the existence of ODC-defects modified by atoms having electronic configuration different from that of IV group elements. The aim of the present work is detection and investigation of the ODC-type defects formed during selenium ion implantation in thin SiO_2 film.

2. Materials and methods

Time-resolved PL spectra in the region of 1.5–6.0 eV, time-resolved PL excitation spectra (3.7–18.0 eV) and the PL decay

* Corresponding author: Tel.:73433759788.
E-mail addresses: a.f.zatsepin@ustu.ru, zats@2-u.ru.(A.F. Zatsepin)

0022-2313/$ - see front matter © 2013 Elsevier B.V. All rights reserved.
http://dx.doi.org/10.1016/j.jlumin.2013.05.041

kinetics were measured at room and low temperatures using synchrotron radiation (SR) on a SUPERLUMI station (Beam-line I, HASYLAB, DESY). Samples were mounted in a sample holder attached to a He-flow cryostat with vacuum not less than 7×10^{-10} Torr. At the storage ring DORIS the full width at half maximum (FWHM) of SR pulses was 130 ps with the repetition period of 192 ns. The 2 m vacuum monochromator (Al-grating, spectral resolution 3.2 Å) was used to excite of the PL in 3.7–18 eV range. The 0.3 m ARC Spectra Pro-300i monochromator equipped with either R6358P (Hamamatsu) photomultiplier was used as a registration system. Time-resolved PLE spectra were measured in two independent time spans $\Delta t_1=21$ ns (the fast component) and $\Delta t_2=72$ ns (the slow component), which were delayed relative to the beginning of the SR-excitation pulse for $dt_1=3.7$ ns and $dt_2=101$ ns respectively. Time-integrated (TI) spectra were recorded within the full time range available between two sequential excitation pulses (192 ns). The excitation spectra were normalized to the same number of SR-exciting photons using sodium salicylate. The PL emission spectra were not corrected to the spectral sensitivity of the recording system.

As samples we have used amorphous, thermally grown SiO_2 layers, 500 nm thick, wet oxidized at 1100 °C on a crystalline Si substrate. The ion implantations of Se^+ were performed with energy of 330 keV, with a uniform dose of 5×10^{16} ions/cm^2. This implantation energy and dose led to an atomic dopant fraction of about 4 at% at nearly the half depth of the oxide layers. The Sn^+-implanted samples with similar characteristics (400 keV, 5×10^{16} ions/cm^2) were used as a reference. A post-implantation thermal annealing for both types of samples was performed at temperature $T_a=900$ °C for 1 h in dry nitrogen. An additional 1 h air annealing at 500 °C was applied to selenium-implanted films in order to investigate the oxidation processes.

3. Results

The ion-implanted and once annealed SiO_2:Se^+ and SiO_2:Sn^+ samples show similar sets of PL bands at the 1.5–3.8 eV region (Fig. 1). The most pronounced maxima for selenium-implanted samples are 2.5 eV (green band) and 3.4 eV (violet band) ones. The violet band demonstrates a weakly pronounced fine structure containing equally spaced oscillations, intensity of which in the time-integrated spectrum, however, is higher than the noise level.

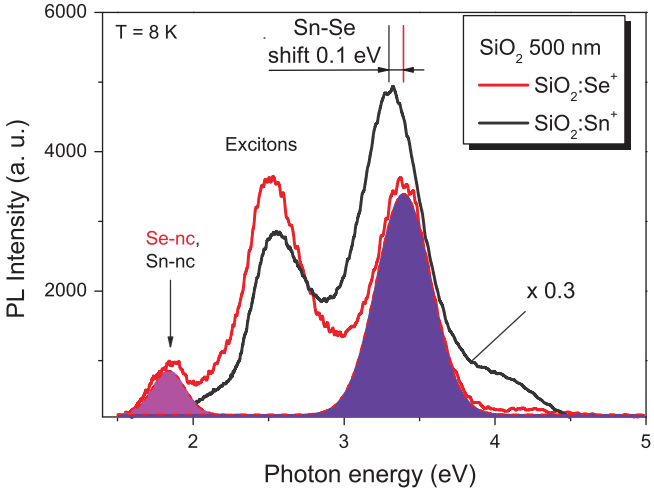

Fig. 1. Time-integrated PL spectra of SiO_2:Se^+ films annealed at $T=900$ °C in N_2 atmosphere registered under 13 eV excitation. Deconvoluted Gaussian components are denoted by dashed lines. A reference spectrum of SiO_2:Sn^+ film (annealed at $T=900$ °C in N_2) is shown by black line. (For interpretation of the references to color in this figure, the reader is referred to the web version of this article.)

These oscillations may correspond to the vibronic states of the luminescent defect.

Besides, there are some weak peaks in the 1.7–2.0 spectral range that may be related to the selenium and tin nanoclusters [2]. In principle, there might be another interpretation of the long wavelength bands appeared due to the possible interactions of synchrotron radiation with the SiO_2 matrix. For example, the band around 1.9 eV is often observed in silica and related to nonbridging oxygen hole centers (NBOHC). Messina et al. [7] have demonstrated that NBOHC may be induced by vacuum UV synchrotron radiation. Determination of their nature requires a detailed research and goes beyond the scope of the present study.

Gaussian deconvolution of the green band reveals two components (2.5 eV and 2.6 eV bands having different halfwidths) responsible for its nonelementary shape. The components may be ascribed to the photoluminescence of self-trapping excitons [11–13], silica point defects or impurity-related centers [8,14]. Contrary, the violet band has truly Gaussian profile. The latter band is implanted ion-specific: as compared to tin-containing films one can observe a 0.1 eV spectral shift of the violet band from 3.3 eV to 3.4 eV in selenium-implanted ones.

The fragment of time-resolved spectra in the 3–5 eV region is shown in Fig. 2. The fast component of spectrum dominates over the slow one in the 4–4.75 eV range, indicating the existence of a weak 4.26 eV band with nanosecond-order kinetics. This maximum loses its intensity with growing temperature (see Fig. 2a, b). At low temperatures the PL lifetime of the 3.4 eV band is more than 200 ns. The room temperature measurements reveal a complex PL decay law for the violet band under high energy excitation

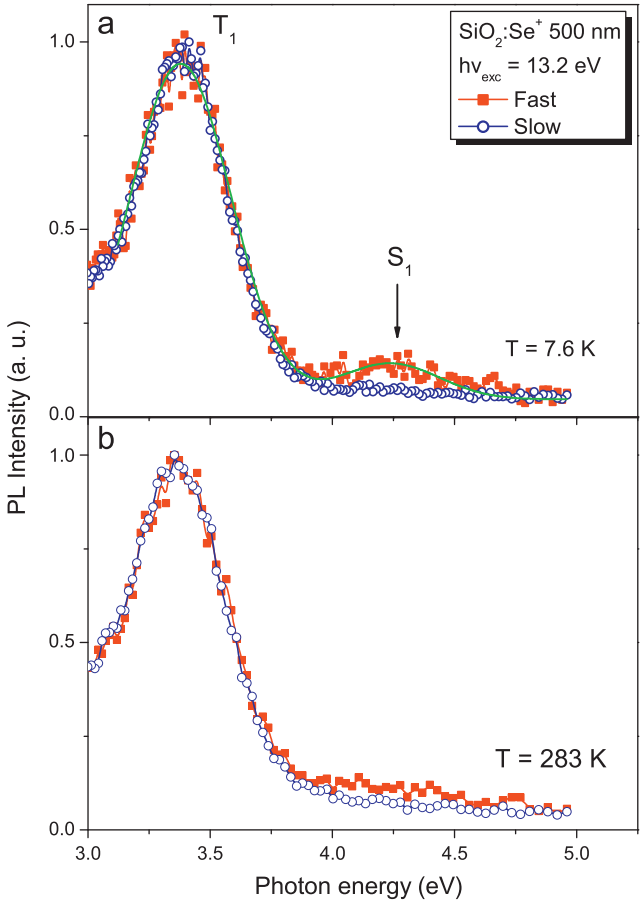

Fig. 2. Time-resolved PL spectra of the SiO_2:Se^+ films at helium (a) and room (b) temperatures recorded under 13.2 eV excitation. The fast and slow components of PL spectra have been normalized to compare their shape.

($h\nu > 10.4$ eV), comprising two exponentials with $\tau_1 = 11.4$ ns and $\tau_2 = 91$ ns (Fig. 3). It can be seen from the Fig. 4a that PL spectrum intensity decreases approximately by 3 times while temperature grows from 8 K to 300 K. The lifetime of the short component is significantly larger than the synchrotron radiation pulse width (see the black curve in Fig. 3) and therefore could not be attributed to instrumental effects.

After the air atmosphere annealing the violet peak loses 70% of its intensity, possibly due to oxidation or defect healing processes. Its width decreases by 0.04 eV and spectral position shifts by 0.05 eV toward higher energies. Both effects may be explained by the passivation of the part of emission centers and corresponding modification of 3.4 eV band nonuniform broadening. Besides, one may notice the 1.85 eV PL band does not shift but becomes narrowed after annealing, probably due to crystallization or redistribution of nanoclusters.

The excitation spectra for green and violet bands (Fig. 4b) have complex shape with several peaks within 4–6 eV (defect-related [15]), 8–11 eV regions and a sharp maximum near 12 eV. Air annealing leads to the smoothing of the entire PLE spectrum. One can notice that the 2.5 eV band is efficiently excited through 10.5 eV and 12 eV PLE maxima related to SiO_2 excitons. Contrary, for 3.4 eV band the 4–6 eV excitation is more intensive and comparable to high energy exciton-related peaks.

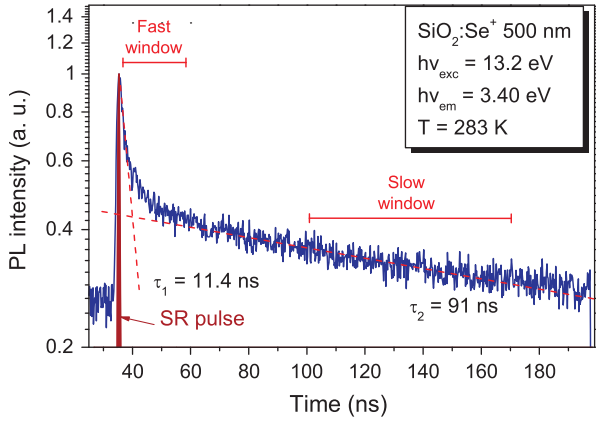

Fig. 3. PL decay kinetics for the 3.4 eV band of SiO_2:Se^+ film at room temperature under 13 eV excitation. The time windows ("fast" and "slow") chosen for time-resolved spectra acquisition are shown. The SR excitation pulse is drawn for comparison. (For interpretation of the references to color in this figure, the reader is referred to the web version of this article.)

4. Discussion

The results of low-temperature, time-resolved studies (Figs. 1–3, Table 1) show that an intensive PL band 3.4 eV appears after ion implantation and additional thermal treatment. The 4–7 eV excitation through the low-energy excited states of the SiO_2 matrix is more efficient for the 3.4 eV band revealing its defect-related nature. Based on several factors we attribute this maximum to a Se-related defect of ODC type. Firstly, a strong effect of air annealing on the violet peak reveals its oxygen deficiency-related nature. Secondly, the occurrence of similar bands in the PL spectra of tin and germanium implanted silica reveals comparable energy structure of the luminescent centers for all these species [9]. Thirdly, the spectral parameters of this band in Se-implanted samples have individual features, despite the proximity of the 3.3 eV band in Sn-doped samples (Table 1). The evidences noted above allow a preliminary interpretation of this band as a triplet luminescence ($T_1 \rightarrow S_0$) of a new defect variant—selenium-related oxygen deficient center.

Analyzing the PL temperature and kinetic dependencies for the new center identified as SeODC triplet PL one may notice the following regularities. The main peculiarity of the energy structure of SeODC is the possibility of triplet (T_1) state excitation under UV and VUV light irradiation with participation of silica matrix excitons. Particularly the 12 eV PLE band, shown in Figs. 5 and 6, is close to the known 11.6 eV absorption band of SiO_2 excitons [16,17]. At the same time the SeODC defect almost does not demonstrate singlet PL excitation. A temperature-driven PL intensity increase (Fig. 4) points out the existence of substantial energy

Table 1
Spectral parameters for the triplet PL band of once (N_2), twice (N_2+air) annealed SiO_2:Se^+ and SiO_2:Sn^+ films.

Sample	SiO_2:Se (N_2)		SiO_2:Se (N_2+air)	SiO_2:Sn (N_2)
Temperature (K)	8	283	8	8
Peak position (eV)	3.39	3.39	3.44	3.32
FWHM (eV)	0.36	0.36	0.31	0.41

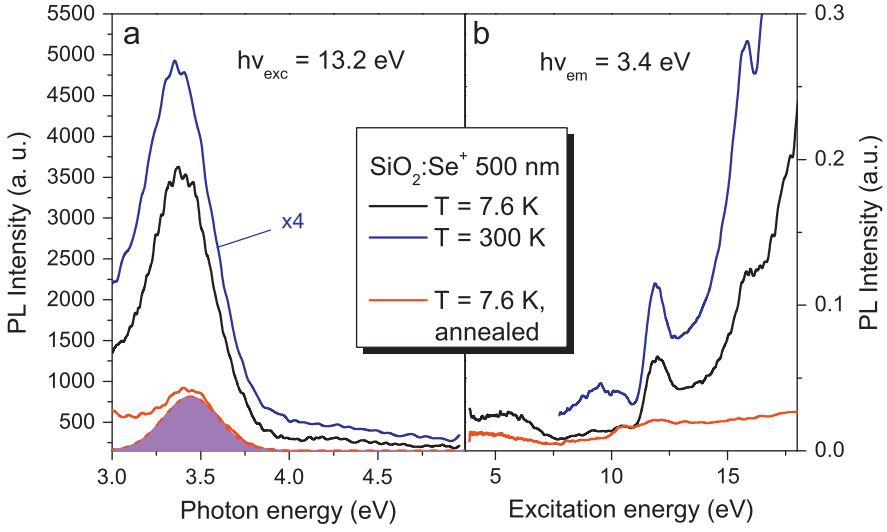

Fig. 4. The effects of registration temperature and additional air annealing on the shape of time-integrated spectra for Se-implanted films: (a) PL and (b) PLE. Air annealing drastically vanishes the 3.4 eV band. (For interpretation of the references to color in this figure, the reader is referred to the web version of this article.)

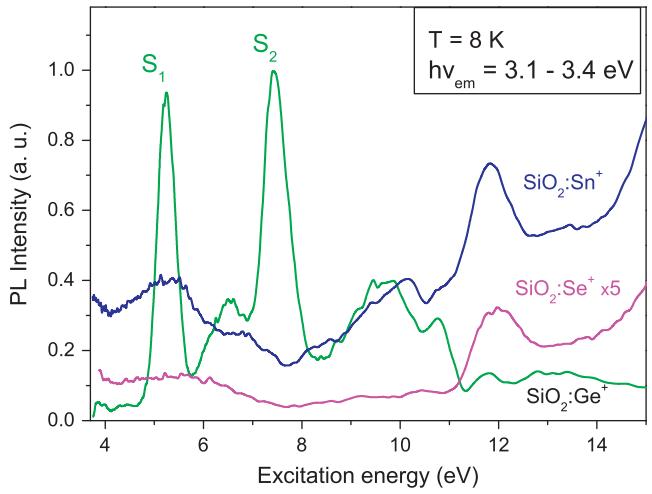

Fig. 5. The comparison of the PL excitation spectra for triplet bands of Ge- [10], Sn- [2] and Se-related ODC in ion-implanted silica films. The figure demonstrates a tendency of falling direct excitation intensity in the row GeODC→SnODC→SeODC. Contrary, the 10–12 eV PLE band arise in the spectra of tin and selenium implanted samples.

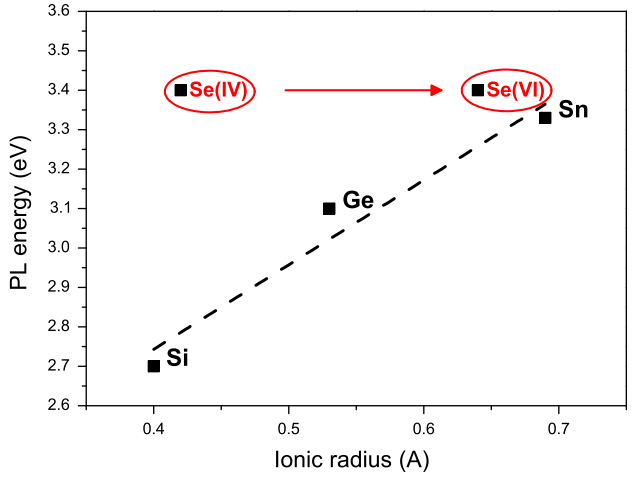

Fig. 6. The correlation between ionic radius and corresponding triplet photoluminescence energy for the known isoelectronic series of Si-, Ge- and SnODC along with possible IV-coordinated and under coordinated hexavalent selenium (=S̈e=). Se(VI) is close to the main correlation trend, both by spectral position and ionic radius.

barrier between the high-energy excited state and the lowest radiative defect level. These features are extraneous for known Si and GeODC, demonstrating efficient singlet excitation, but are akin to that of SnODC (Figs. 1 and 5) found in thin films.

Silicon, germanium and tin-related oxygen deficient centers are well known to have triplet luminescence bands with lifetimes decreasing from 10.1 ms (Si) to 113 μs (Ge) and 10.1 μs (Sn) [5]. At helium temperatures the 3.4 eV PL band has more than 200 ns lifetime, so the selenium-related ODC is close to the tin-related variant. A heating up to room temperatures further accelerates the decay of the SeODC triplet photoluminescence to nanosecond range (Fig. 3). Similar effect was observed by Canizzo et al. [6,9] for SnODC singlet PL bands. In our case the time-resolved excitation spectra for fast (11 ns) and slow (91 ns) decay components are identical. This fact indicates that they belong to the same emission center. Both components appear at high temperatures, where the PL quenching processes take place. Presently the nature of the fast decay component (11 ns) is not known and requires special investigations. Taking into account the complex processes of SeODC PL thermal quenching at room temperatures we attribute the slow component (91 ns) to ODC triplet–singlet transition. Thus one may draw a tendency of decreasing ODC triplet PL lifetime in the Si→Ge→Sn→Se row. It might be assumed that the heavy cation distorts the silica lattice surrounding ODC defect, hence modifying the overall center energy structure.

Indeed, though the emission bands energies are quite close for Ge-, Sn- and SeODC, it could be seen from Fig. 5 that the PL excitation spectrum depends on the type of cation. The SiODC and GeODC both in silica films and glasses have sharp and intensive excitation bands corresponding to the first and second singlet excited states [18,19]. At the same time these features are weak in case of SnODC and almost completely blurred for selenium implanted films. Instead, there are pronounced excitation bands at silica excitons region 12 eV (Fig. 5) for Sn- and SeODC, while for silicon and germanium-related defects such exciton-mediated channel is inefficient. The singlet luminescence 4–4.5 eV disappears in the same manner: it is pronounced for GeODC, weak but detectable at 4.1 eV for tin-related defects and is almost absent for SeODC (Figs. 1 and 2). Thus we believe the new selenium-related center is very close to SnODC by its excitation mechanism. In other words these facts suggest that the size factor might be more influential for the spectroscopic features than the similarity of outer electronic shell.

The analogy drawn between impurity-related ODCs and Se-containing defect allows a possibility of silicon substitution by selenium in the SiO_2 lattice. From the structural point of view both the atomic mass (78.96 amu) and ionic radius (0.42 Å [15]) in the four-coordinated state for tetravalent Se(IV) are less than that for Sn(IV) (118.71 amu and 0.69 Å, respectively [20]), so an easy incorporation of the Se atoms into the SiO_2 lattice may be imagined. Just as it is accepted for other impurity-related ODCs [18,19], in case of Se(IV) one can assume two structural models for SeODC: either twofold selenium =Se: or oxygen vacancy ≡Si–Se≡ or ≡Se–Se≡. It is worthy of note that the Se–Se bonds in the films under study were registered earlier by means of Raman spectroscopy [21]. Fig. 6 shows the main correlation trend of ionic radius versus triplet PL energy for isoelectronic series of Si-, Ge- and SnODC.

Photoluminescence energy demonstrates a blue shift with growing cation radius in these defects. It can be seen that a hexavalent Se(VI) atom with an equilibrium coordination number of 6 has an ionic radius (0.64 Å [20]) close to that of Sn(IV). Though selenium is not an isoelectronic analog of the group IV elements, it fits well to the correlation trend described. Forming an oxygen deficient site, such Se atom can have four oxygen bonds along with two unshared electrons [20]. Similar case was observed for dense SiO_2 modifications where ODC-like luminescence was formed by defective octahedral motifs [22]. So we suggest the =S̈e= defect as a model for the possible SeODC.

The overall picture of the selenium ODC defect proposed by this article is presented in Fig. 7. The most efficient excitation is performed under VUV (12 eV) irradiation and results in energy transfer from the matrix excitons to the higher excited states of the defect. The energy is further transferred to the triplet state T_1 through a small potential barrier which causes the temperature dependence of the 3.4 eV $T_1 \rightarrow S_0$ photoluminescence (final relaxation stage, see Fig. 3).

The weak PL band at 4.2 eV could be related to the singlet–singlet transition within the proposed SeODC model. Fast PL kinetics observed in this spectral region support such attribution. The transition from the higher excited states to S_1 state of SeODC is non-radiative and probably requires thermal activation with a high energy barrier, which explains the weakness of singlet luminescence observed. From the time-resolved spectra (Fig. 2a) one can see that the 4.2 eV PL peak has nanosecond order kinetics.

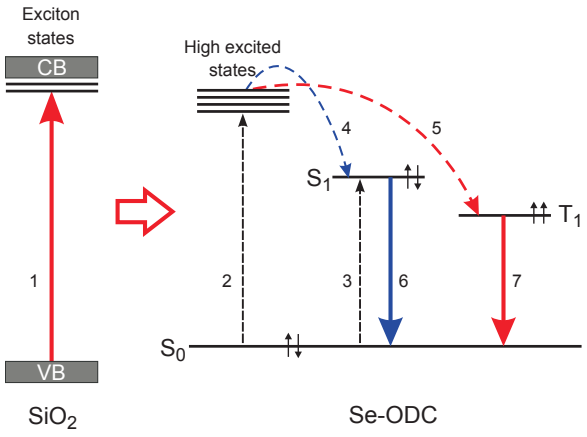

Fig. 7. Energy scheme of the SeODC center, involving singlet (S_1, S_0) and triplet (T_1) excited states. Possible intermediate excited states (either defect or matrix-related) are presented. 1, 2, 3—optical excitation; 4—high-barrier transition; 5—low-barrier transition; 6, 7—radiative relaxation. The most active excitation path includes VUV irradiation with silica excitons generation, energy transfer to the high excited states and final triplet–singlet transition (marked by red color). Both direct and indirect ways of excitation of S_1 singlet state are not efficient.

However the low intensity of the 4.2 eV maximum does not allow determining the precise value of PL lifetime.

5. Conclusions

The results obtained allow to conclude that the violet PL band appears as a consequence of the silica matrix structure change during ion implantation and is related with oxygen deficiency. Based on the comparative analysis of the spectroscopic features of the isoelectronic Si, Ge and SnODC defect series, the violet band is attributed to triplet–singlet transition of the Se-related ODC. The energy structure of the new center causes weak singlet PL excitation and emission bands. However an efficient VUV excitation channel of the triplet state was found, which involve silica excitons-aided energy transfer to intermediate excited states.

By spectral and kinetic parameters the new variant of ODC considerably differs from the Si- and Ge-related defect centers, but is close to SnODC. Taking into account the ionic radii values of the noted elements it may be concluded that the size is the main factor determining the ODC luminescent properties. Based on this principle we proposed a preliminary model of SeODC defect as a four-coordinated hexavalent Se atom within the SiO_2 lattice.

Acknowledgments

The work was partially supported by RFBR Projects 13-08-00568, 13-02-91333, DFG Project FI 497/15-1 and HASYLAB (DESY) Project I-20110043.

References

[1] J.Z. Zhang, Optical Properties and Spectroscopy of Nanomaterials, World Scientific, 2009.
[2] A.F. Zatsepin, E.A. Buntov, V.S. Kortov, V.A. Pustovarov, H.-J. Fitting, B. Schmidt, N.V. Gavrilov, X-ray, Synchrotron Neutron Tech 6 (2012) 668.
[3] L. Rebohle, J. von Borany, W. Skorupa, H. Frob, S. Niedermeier, Appl. Phys. Lett. 77 (2000) 969.
[4] A.F. Zatsepin, H.-J. Fitting, V.S. Kortov, V.A. Pustovarov, B. Schmidt, E.A. Buntov, J. Non-Cryst. Solids 355 (2009) 61.
[5] L. Skuja, J. Non-Cryst. Solids 239 (1998) 16.
[6] A. Cannizzo, M. Leone, R. Boscaino, A. Paleari, N. Chiodini, S. Grandi, P. Mustarelli, J. Non-Cryst. Solids 352 (2006) 2082.
[7] F. Messina, L. Vaccaro, M. Cannas., Phys. Rev. B 81 (2010) 035212.
[8] L.N. Skuja, J. Non-Cryst. Solids 149 (1992) 77.
[9] A. Cannizzo, S. Agnello, M. Cannas, N. Chiodini, M. Leone, A. Paleari, J. Non-Cryst. Solids 351 (2005) 1937.
[10] T. Hayakawa, T. Enomoto, M. Nogami, J. Mater. Res. 17 (2002) 1305.
[11] A.N. Trukhin, J. Non-Cryst. Solids 149 (1992) 32.
[12] A.N. Trukhin, M. Goldberg, J. Jansons, H.-J. Fitting, I.A. Tale, J. Non-Cryst. Solids 223 (1998) 114.
[13] E. Vella, F. Messina, M. Cannas, R. Boscaino, Phys. Rev. B 83 (2011) 174201.
[14] J. Choi, B. Park, Y. Choi, J. Heod, W. Chung, J. Non-Cryst. Solids, http://dx.doi.org/10.1016/j.jnoncrysol.2012.12.016 (2013).
[15] A.F. Zatsepin, E.A. Buntov, V.S. Kortov, D.I. Tetelbaum, A.N. Mikhaylov, A. I. Belov, J. Phys.: Condens. Matter 24 (2012) 045301.
[16] A.N. Trukhin, in: G. Pacchioni, L. Skuja, D.L. Griscom (Eds.), Defects in SiO_2 and Related Dielectrics: Science and Technology, Kluwer Academic, New York, 2000.
[17] S.T. Pantelides, in: S.T. Pantelides (Ed.), The Physics of SiO, and Its Interfaces, Pergamon, Oxford, 1978.
[18] A.F. Zatsepin, V.S. Kortov, H.-J. Fitting, J. Non-Cryst. Solids 351 (2005) 869.
[19] N. Chiodini, F. Meinardi, F. Morazzoni, A. Paleari, R. Scotti, D. Di Martino, J. Non-Cryst. Solids 261 (2000) 1.
[20] R.D. Shannon, Acta Cryst. A32 (1976) 751.
[21] A.F. Zatsepin, E.A. Buntov, V.S. Kortov, H.-J. Fitting, Yu.S. Ponosov, Bull. Russ. Acad. Sci. Phys. 74 (2010) 201.
[22] A.N. Trukhin, J. Non-Cryst. Solids 357 (2011) 1931.